

# High/Low Spin emission Spectra

Alessandro Foligno, University of Pisa, Scuola normale superiore  
Supervisors: Maria Naumova, Sophie Canton

September 5, 2019



## Abstract

The aim of the project was eventually to characterize high and low spin states of  $\text{Ni}^{2+}$ , focusing in particular on how the X-ray emission spectra (Xes) looks like in the two cases.

## Contents

<b>1</b>	<b>Introduction</b>	<b>2</b>
<b>2</b>	<b>Xes</b>	<b>2</b>
<b>3</b>	<b>Multiplet Theory</b>	<b>2</b>
3.1	LS coupling	3
3.2	Coulomb and exchange integral [1]	3
3.3	$\text{Ni}^{2+}$	4
3.4	Perturbation Theory	5
3.5	Limits of perturbation theory	5
3.6	Dipole transition	6
<b>4</b>	<b>Crystal field</b>	<b>6</b>
4.1	Octahedral Field	6
4.2	$D_{4h}$ Symmetry	7
4.2.1	Crystal field parameters values	7
<b>5</b>	<b>CTM4XAS</b>	<b>7</b>
<b>6</b>	<b>Energy levels in the 2p1s transition</b>	<b>9</b>
6.1	$K_{\alpha 1}$ edge	9
6.1.1	$K_{\alpha 2}$	10
6.2	Crystal field	12
6.2.1	$K_{\alpha}$	12
6.2.2	$K_{\beta}$	12
6.3	Crystal field parameters for high-low spin state	14

<b>7</b>	<b>fit results</b>	<b>18</b>
7.1	Ni(Pc) . . . . .	18
7.1.1	$K_\beta$ emission lines . . . . .	18
7.1.2	$K_\alpha$ emission lines . . . . .	20
7.2	Ni(Terpy) <sub>2</sub> . . . . .	21
7.2.1	$K_\beta$ emission lines . . . . .	21
7.2.2	$K_\alpha$ emission lines . . . . .	21
<b>8</b>	<b>ORCA programm</b>	<b>23</b>

# 1 Introduction

In this document, I will present the work done during this month at Desy. In section 2 I briefly explained the Xes emission processes.

Then, I learned about Multiplet theory and what role it has in the structure of the spectra generated by various optical processes, such as Xas and Xes, with particular attention to how compute effectively the interaction terms between electrons exploiting group theory.

Then, in section 3, I focused on crystal field theory and how different simmetries in metal complexes can give rise to different splitting of the electron degenerate levels.

In section 5 I tried to study the lines arising from the multiplet structure of nickel.

In the end I concentrated on how the crystal field can force an atom into a low spin configuration and what the spectra looks like depending on the spin, section 5.3.

I eventually tried to fit the experimental data of high/low spin compounds with the predicted spectra in section 6, obtaining unexpected results for a compound which should be in a high spin state but looks like in low spin one.

# 2 Xes

X-Ray Emission Spectroscopy (XES) is often referred as a second-order optical process, because it occurs after the excitation of a core  $1s$  electron (tipically, but the electron can also be stripped from a  $2p$  orbital), that is stripped away from the atom.

Following this 1-st order process, there can be the decay of an electron from  $p$  shells (according to selection rules) with consequent emission of a photon.

The Xrays emitted in this way are then measured with some detector.

The project focused, in particular, on the Xes spectrum of various  $\text{Ni}^{2+}$  compounds, so in this report I will eventually always refer to this atom.

In this case, there are 2  $p$ -transitions that emit in the Xray range; that is  $1s \rightarrow 2p$  and  $1s \rightarrow 3p$

To simulate (and fit) these spectra I used the CTM4XAS program.

# 3 Multiplet Theory

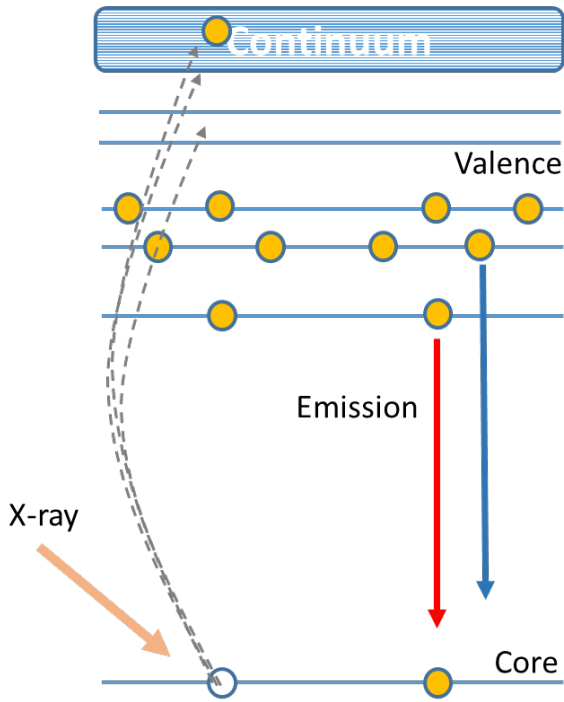
The basic assumption for dealing with multi-electon system in atomic physics is considering that electrons around the atom fill progressively all the shells, that is, some states with fixed orbital angular momentum. When a shell is complete, it has spherical symmetry and its effect is to "change" the nucleus charge.

So the idea is to focus mainly on a single shell until it is filled. If we make the brutal approssimation of independet electrons, thus ignoring electron- electron repulsion, or computing it perturbatively, then for an angular momentum of, let's say,  $l$ , there are  $2 \cdot (2l + 1)$  states that can be occupied. This is because electrons have also the spin quantum number, that can be valued  $\pm \frac{1}{2}$ .

The Hamiltonian for an incomplete shell looks like this:

$$H = \frac{\hbar^2}{2m_e} \sum_i \nabla_i^2 + V_{eff}(r) + \sum_{i,j} \frac{e^2}{|\vec{r}_i - \vec{r}_j|}$$

Where we have included the interaction with the other closed shells in the form of an effective potential. This hamiltonian is invariant under rotations of all the electrons, which means that it commutes with the *total* angular



momentum that is thus a good quantum number. So, different configurations with the same number of electrons in a closed shell, can be labeled with different total angular momentum, which then defines a multiplet.

For example, let's suppose to have two electron in a  $d$  shell, which means  $l = 2$ .

The tensor product representation  $2 \otimes 2$  can be decomposed in 5 irreducible representation, that are  $L = 0$ ,  $L = 1$ ,  $L = 2$ ,  $L = 3$ ,  $L = 4$  of which the one with an even angular momentum are symmetric under electron exchange and the ones with an odd angular momentum are antisymmetric.

Those that are symmetric force the spin in the singlet ( $S = 0$ ), the ones antisymmetric are instead in a spin triplet  $S = 1$ . Using as labels total spin (but writing instead of the spin the multiplicity  $2S + 1$ ) and orbital momentum of the shell (written with the atomic  $S P D \dots$  notation), the multiplet structure in the example is:

$$^1S, ^3P, ^1D, ^3F, ^1G, \quad (1)$$

The idea behind the calculation is, instead of considering single-electron state, to use the whole multiplet for calculations because it is already an eigenspace of the perturbative Hamiltonian which includes electron interaction. A more detailed example is given in [3.4](#)

### 3.1 LS coupling

Until now, spin and orbital momentum have been considered as independent quantum degrees of freedom that don't interact and are conserved separately, hence as good quantum numbers; this isn't actually true. For many atom there's an effect called spin-orbit coupling (LS coupling) that can be thought as one more (little) term in the Hamiltonian in the form:

$$\Delta H_{LS} = A (\vec{L} \cdot \vec{S})$$

In this way the, hamiltonian only commutes with the total angular momentum  $\vec{J} = \vec{L} + \vec{S}$  that is a good quantum number.

For example, the multiplet  $^3P$  has  $S = 1$  and  $L = 1$  and so 3 possible values of  $J = 0, 1, 2$ . Hund's rule states that for a shell that is less than or half-full,  $J$  takes its lower absolute value, that in this case would be 0. If the shell is more than half-full, then it takes its maximum value.

The spin-orbit coupling is stronger for heavier atoms, and in particular for electrons close to the center.

### 3.2 Coulomb and exchange integral [\[1\]](#)

What the program CTM4XAS does, to calculate the energy of each multiplet, is to compute the interaction between each couple of electrons. Considering the fact that the wavefunction of many electron systems is to be antisymmetric,

the interaction energy is:

$$E_{\text{interaction}} = \frac{1}{2} \sum_{i,j} \langle i, j | \frac{e^2}{|\vec{r}_i - \vec{r}_j|} | i, j \rangle - \langle i, j | \frac{e^2}{|\vec{r}_i - \vec{r}_j|} | j, i \rangle$$

The latter term is called exchange integral and arises only from the fact that electrons wavefunction is antisymmetric.

Since these terms are invariant under collective rotations of all the electrons, they can be decomposed in spherical armonics the following way:

$$\frac{1}{|\vec{r}_i - \vec{r}_j|} = \sum_{l=0}^{+\infty} \frac{4\pi}{2l+1} \sum_{m=-l}^l Y_{l(\theta_i, \phi_i)}^{m*} Y_{l(\theta_j, \phi_j)}^m \frac{r_{<}^l}{r_{>}^{l+1}} \quad (2)$$

Where  $r_{<}$  refers to the minimal radius between  $i$  and  $j$ , and vice-versa.

Instead of the spherical armonics, one often finds the function

$$C_l^m = \sqrt{\frac{4\pi}{2l+1}} Y_l^m$$

Restricting to a shell, the wavefunction is of the form:

$$\psi_m = R_{(r)} Y_{l(\theta, \phi)}^m$$

And the radial part  $R_{(r)}$  is the same for all the electron in the shell (also called *equivalent electrons*), the only things that can vary for them are the  $m$  and the spin quantum number.

Thus, the only integrals one has to compute for a general interaction between two electrons are:

$$c_{l1, l2, m1, m2, l', m'} \langle C_{l1}^{m1} | Y_{l'}^{m'} | C_{l2}^{m2} \rangle = \int \left( C_{l1}^{m1}(\theta, \phi) \right)^* Y_{l'}^{m'}(\theta, \phi) C_{l2}^{m2}(\theta, \phi) d\phi d\theta$$

and the radial part:

$$R_{n1, l1, n2, l2, l'} = \int R_{n1, l1}^* r^{l'} R_{n2, l2}$$

Where selection rules impose, for the angular part:

$$|l_1 + l_2| \geq l'$$

$$m_2 + m' = m_1$$

And parity selection rules impose that the parity of  $l_1 + l_2$  is equal to the parity of  $l'$

### 3.3 Ni2+

Let's calculate the multiplets of the nichel<sup>2+</sup>: it has a partially filled  $d$  shell:

$$1s^2 2s^2 2p^6 3s^2 3p^6 3d^8$$

We can imagine that actually the  $d$  shell is complete, but it has 2 holes in it, which behave like "positive" charged electrons. So the possible spectral terms are the ones found in [1](#):

$$^1S, ^3P, ^1D, ^3F, ^1G$$

Hund's rule states that the ground state has the highest angular momentum between the states with the highest spin, so it's the  $^3F$ . Since the shell is more than half-filled, the  $J$  quantum number is to be the highest to get the lowest energy, so the spectral term is:

$$^3F_4$$

In the Xes process, a hole is created in the  $s$  shell, and is then moved with a Xray decay in the  $p$  shell. To calculate the energy of the possible final states, one has to calculate the interaction between the hole in the  $p$  shell with the valence electrons in the  $d$ . There are two kind of radial integrals to make: Coulomb and Exchange.

Let's focus on the Coulomb integral: in the expansion [2](#) only the terms with even  $l$  are allowed because of parity(thanks

to rule 3.2 ) and only for  $l \leq 2$  because the  $p$  shell only allows  $l' \leq |l_1 + l_2| = 2$  . So in the end we have 2 radial integrals to make, these are called  $F^k$  with  $k = 0, 2$  in this case.

The integrals of the angular part are tabulated and they are collected under the factor  $f_k$  with  $k = 0, 2$ . So in the end the interaction is :

$$\sum_k f_k F^k = f_0 F^0 + f_2 F^2$$

The radial integrals can be evaluated using and Hartree Fock code. For the exchange integral, instead, since the parity of  $p + d$  is odd,  $k$  can take only odd values that are less than  $\leq p + d = 1 + 2 = 3$ . The exchange integrals are indicated with the letters  $G$  and  $g$  (for radial and angular part respectively).

$$\sum_k g_k G^k = g_1 G^1 + g_3 G^3$$

These integrals are often scaled with a factor of about 80% because they are calculated by the codes in the unperturbed atom, whereas if there's a core hole, all the states are shrunk towards the center and this somehow changes the operators expectation values of some factor. [2]

### 3.4 Perturbation Theory

The question is: how does the program compute all the radial integrals of the previous section(the angular part are tabulated and can be found analytically)? What wave function does it use? The answer is the unperturbed wave function of the atom, neglecting all the interaction between electron of the same shell.

Then, on these wavefunction it uses perturbation theory(all the electron of unfilled orbitals have to be considered). Perturbation theory states that a small potential  $\delta V$  added to the Hamiltonian gives rise to a shift in energy:

$$\Delta E = \langle i | \delta V | i \rangle$$

Where the states are the *unperturbed states*. If there is some degeneracy, one has to consider the matrix:

$$V_{ij} = \langle i | \delta V | j \rangle$$

And diagonalize it to find the energy eigenvalues. In our case, states are multielectron states, so for example for the  $Ni^{2+}$  ground states, which has 2 holes, one has to compute all the:

$$\binom{10}{2} = 45$$

energy levels for all the possible configuration (one can arrange the first hole in 10 states, the second in 9 states and then divide by two because they are indistinguishable).

This is where multiplet theory comes in help, because the single-electron states are part of a  $J = 2$  representation, their tensor product creates  $J = 0, J = 1, J = 2, J = 3, J = 4$  multiplets (for two hole configurations). So in the end, there are only 5 degenerate energy levels, and not 45.

Let's check the number of states is 45. Every representation has multiplicity  $2j + 1$ , but spin has also to be taken into account, and the  $J$  even states are in a singlet of spin, the odd  $J$ s are in a triplet, which means their multiplicity has to be multiplied by 3:

$$1 + 3 \cdot 3 + 5 + 7 \cdot 3 + 9 = 1 + 9 + 5 + 21 + 9 = 45$$

A similar job must be done to calculate the interaction of the  $d$  shell with the  $p$  hole in the final state.

The program then adds to these electronic interaction the crystal field (which will be discussed later) and then diagonalizes the whole matrix to find the proper energy levels.

### 3.5 Limits of perturbation theory

The assumption that the electron states are unperturbed is valid as long as their next term in perturbation theory is negligible. This is:

$$|\delta \Psi_i\rangle = \sum_j |\Psi_j\rangle \frac{\langle \Psi_j | \delta V | \Psi_i \rangle}{E_i - E_j}$$

So the perturbation has to be little *with respect to the other shells' energies*.

In the case of the  $d$  shell of nickel this might be problematic because the empty  $4s$  shell is very close to it in energy.

### 3.6 Dipole transition

Apart from computing the final and initial energy of the states allowed, one has also to calculate the rate (i.e. the cross section) of the process. This is done by using the Fermi golden rule. For weak field, the interaction of the atom with an external electric field is

$$H = -\vec{d} \cdot \vec{E}$$

Where  $\vec{d}$  is the electric dipole operator

$$d = \sum_i -e\vec{r}_i$$

Then Fermi golden rules states:

$$\sigma_{a \rightarrow b} = \frac{(2\pi)^3 \nu}{\hbar c^2} \frac{1}{c} \left( \vec{d}_{ab}^2 \right) g_b$$

So in principle the program has also to calculate the dipole between the initial and the final state, which is possible within the frame of the HF calculations. The important fact is that the dipole operator has non-null elements only within states that differ for total angular momentum:

$$\Delta J = \pm 1, 0$$

or just orbital angular momentum in absence of LS coupling

The transition are not thin lines, because the Heisenber uncertainty principle for energy states that

$$\Delta E \cdot \tau \geq \hbar$$

Where  $\tau$  is the decaying time of the state. So if the state has a certain rate  $R = \frac{1}{\tau}$  to decay into something else, the energy uncertainty is  $\Delta E = \Gamma = \frac{\hbar}{\tau}$  that is actually the lorentian broadening of the line. Since the initial state is an  $s$  state that has spherical symmetry, the decaying rate is always the same and the lorentian broadening should in principle be equal for the  $K_\alpha$  and  $K_\beta$  emission lines.

## 4 Crystal field

In many compounds, since the atom of nickel is not isolated, there is loss of spherical symmetry. However, the atoms of the molecule can arrange themselves in such a way that some kind of symmetry is maintained. One can account for this effect adding an external potential which possesses the same symmetry of the molecule.

One can add this piece of hamiltonian perturbatively, so remaining in the subspace of the electron shell (an irreducible representation of  $SO(3)$ ).

### 4.1 Octahedral Field

Let's treat the case of the octahedral field. The most general operator inside an irreducible representation can be written as a polynomial of the components of  $\vec{L}$  operator for Wigner-Eckart theorem Restricting to a  $d$  shell, which is the case of Nickel, only the power of  $L$  lower than 4 = 2 + 2 are not null. In [1] it is found that there's only one  $O_h$  identity representation (apart from a simple scalar) inside a  $SO(3)$   $d$  representation, that can have the following Operatorial representation:

$$V_{Oh} = D_q \left( \frac{35}{12} L_z^4 - \frac{155}{12} L_z^2 + 6 + \frac{5}{24} L_+^4 + \frac{5}{24} L_-^4 \right) + \epsilon_0$$

where  $D_q$  is a parameter to be determined experimentally; this Hamiltonian is invariant under  $O_h$  symmetry,  $\epsilon_0$  gives a uniform shift in energy (this is actually a 1st order perturbative approach, valid as long as the field isn't too strong)

This potential causes a split in the  $d$  degenerate energy levels, in fact there are 2 irreducible representation, called by standard notation  $E_g$  and  $T_g$ .

$$E_g = \{ |2, 0\rangle, \frac{1}{\sqrt{2}}(|2, 2\rangle + |2, -2\rangle) \} \quad E = 6D_q$$

$$T_g = \{ |2, 1\rangle, |2, -1\rangle, \frac{1}{\sqrt{2}}(|2, 2\rangle - |2, -2\rangle) \} \quad E = -4D_q$$

The split is equal to  $10D_q$  so the energy levels, neglecting the uniform split, are  $-4D_q$  and  $6D_q$ . Thus the center-of-mass rule is still valid.

## 4.2 $D_{4h}$ Symmetry

From the ideal  $O_h$  symmetry, one can go lower in the  $D_{4h}$  symmetry; this is the symmetry of a deformed octahedral along the  $z$  axis; this means we can add any piece that is invariant for  $L_z$  (rotations by the  $z$  axis) to get the most general  $D_{4h}$  symmetric field. Inside a  $d(l=2)$  representation, the most general piece to add is of the form

$$V_T = AL_z^4 + BL_z^2 + C$$

(the odd powers are null because of parity).

In term of the most used field parameters  $D_t$  and  $D_s$  it is:

$$V_T = D_s(L_z^2 - 2) - D_t\left(\frac{35}{12}L_z^4 - \frac{155}{12}L_z^2 + 6\right)$$

the representation are further split. Thus, the total field is (neglecting the  $\epsilon_0$  contribution which gives a uniform shift):

$$V_T = D_q\left(\frac{35}{12}L_z^4 - \frac{155}{12}L_z^2 + 6 + \frac{5}{24}L_+^4 + \frac{5}{24}L_-^4\right) + \epsilon_0 + D_s(L_z^2 - 2) - D_t\left(\frac{35}{12}L_z^4 - \frac{155}{12}L_z^2 + 6\right)$$

$$V = D_q\left(\frac{35}{12}L_z^4 - \frac{155}{12}L_z^2 + 6 + \frac{5}{24}L_+^4 + \frac{5}{24}L_-^4\right) + D_s(L_z^2 - 2) - D_t\left(\frac{35}{12}L_z^4 - \frac{155}{12}L_z^2 + 6\right) \quad (3)$$

The group  $D_{4h}$  has five representation: 2 are the identity representation and the sign representation,  $a_{1g}, a_{2g}$ , 2 more are 1 dimensional called  $b_{1g}$  and  $b_{2g}$  and there's only one which is 2 dimensional,  $e_g$ . The representation of  $O_h$  in  $d$  orbitals are so split:

$$E_g \rightarrow a_{1g} + b_{1g}$$

$$T_g \rightarrow b_{2g} + e_g$$

The orbitals and the single electron energies are found in Table 1

Energy level	$D_q$	$D_s$	$D_t$	Orbital
$b_{1g}$	6	2	-1	$d_{x^2-y^2} = \sqrt{\frac{1}{2}}(Y_2^{-2} + Y_2^2)$
$a_{1g}$	6	-2	-6	$d_{z^2} = Y_2^0$
$b_{2g}$	-4	2	-1	$d_{xy} = \sqrt{\frac{1}{2}}\frac{Y_2^{-2} - Y_2^2}{i}$
$e_g$	-4	-1	4	$d_{xz \text{ or } yz} = \sqrt{\frac{1}{2}}\Re(Y_2^{-1} \mp Y_2^1)$

Table 1: Table of the energy levels for a single electron in a  $D_{4h}$  field

### 4.2.1 Crystal field parameters values

The next step is to find these parameters on the internet so that I can simulate the spectra using CTM4XAS. This is what I found:

Complex Name	$D_q$	$D_s$	$D_t$	Slater Integral prefactor ( $\pm 0.05$ )
General for porphyrine [3]	0.31	0.31	0.25	—
NiPc [4]	0.27	0.37	0.22	0.75
NiOEP (Octaethylporphyrin) [4]	0.23	0.38	0.23	0.77

## 5 CTM4XAS

The program is actually an interface that uses the code developed by Theo Thole and that calculates the L-edges and Xas and emission lines for Xes processes for various substances. The usual approach would be to use a usual  $DFT$  ab-initio calculation, but this doesn't work for  $L$  edges or for Xes because of the strong overlap of the  $p$  orbitals with the valence  $d$  orbitals.

The program uses a semiempirical approach, meaning that it has all the values of the exchange integrals (or of the Crystal field, that can be given as an input) so it can construct the matrix of the states to diagonalize to find the lowest energy ones.

The program can automatically plot the result using matlab standard plotting library, which takes as input lorentian and gaussian broadening (in  $eV$ ) of the lines. What it does then, is to put a Voigt profile (a convolution of a gaussian and lorentian distribution) on each of the spectral transition lines it has calculated.

The output files include a *\_sticks.xy* file that contains the lines of the transition, and a *.xy* file that contains the profile plotted. They are only present when the autoplot and option is active (for the second file) and the suppress stick option is off (for the sticks file).



## 6 Energy levels in the 2p1s transition

In this section, I try to label the spectral lines that can be seen from a Xes  $1s \rightarrow 2p$  transition, without any crystal field.

The  $K_\alpha$  adsorption lines is split because of L-S coupling of the  $p$  orbital in two distinguishable peaks, named respectively (with increasing energy)  $K_{\alpha 1}$  and  $K_{\alpha 2}$ .

### 6.1 $K_{\alpha 1}$ edge

Let's analyze the peaks on the left; they arise from the coupling of  $p_{\frac{1}{2}}$  with the valence outer multiplet (the ones on the left are the  $p_{\frac{3}{2}}$  core hole).

The valence multiplets states allowed for the final states are:

$$^1G_4 \ ^3F_4 \ ^1D_2 \ ^3P_2 \ ^1S_0$$

Each of these, when coupled with  $p_{\frac{1}{2}}$ , is split in a doublet, except for the  $^1S_0$ , which remains a singlet.

Here, for "coupling" of two shells, I mean the tensor product of the multiplets describing the two shells. In fact, since the interaction between the two shell is invariant under global rotations, each energy level can be labeled with his total angular momentum (of the  $p$  shell multiplet+ the  $d$  shell multiplet).

When doing the tensor product of a  $J = \frac{1}{2}$  representation (the  $p$  multiplet), with another representation  $J \geq \frac{1}{2}$ , one always obtains 2 representation:  $J \pm \frac{1}{2}$ .

The only exception is of course  $J = 0$ .

In our case, then, there are 9 energy levels possible for the final state: two for each valence multiplet except for the  $S$  multiplet.

But, because of selection rules and the absence of L-S coupling on the valence orbital (the electrons in the  $d$  shell are very far away from the center), in the end there are only few allowed transitions. In practice, the only allowed valence final levels are the high spin ones:

$$^3F \text{ and } ^3P$$

The  $^3P$  can only be reached in case of a coupling with the  $p$  core hole, because selection rules only allow for  $\Delta J_{tot} = \pm 1, 0$ . The initial state has  $^3F$  on the valence shell and  $J = \frac{1}{2}$  on the  $s$  shell hole, which means two possible initial angular momentum  $\frac{5}{2}$  and  $\frac{7}{2}$  (that have the same energy!).

Looking instead at the final states, when the  $P$  valence multiplet couples with the  $p_{\frac{1}{2}}$  core hole (that has  $J = \frac{1}{2}$ ), it creates two levels with total angular momenta  $1 \pm \frac{1}{2}$ . Of these, only the  $J_{tot} = \frac{3}{2}$  can be reached from the initial  $J_{tot} = \frac{5}{2}$ . Instead, the  $^3F$  has two final states that can both be achieved by dipole selection rules:

$$J_{final} = 2 \pm \frac{1}{2}$$

These are thus the two main peaks, and they are reduced to only one peak reducing the interaction with the  $p$  shell (slater  $Fpd$  and  $Gpd$  parameters). These can be observed in picture 1

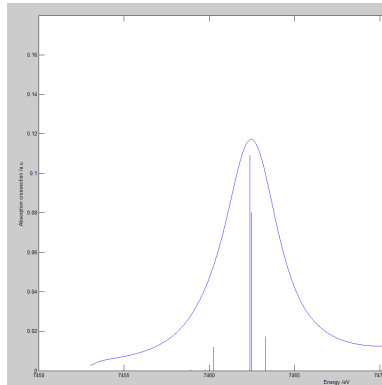


Figure 1: The two main peaks are the  $F$  multiplets, on the right to them there's the  $P$  multiplet

### 6.1.1 $K_{\alpha 2}$

Let's focus on the peaks on the right; to make it short I only consider the highest peaks. To quickly find the levels which have final valence configuration  $^3F_4$ , turn off p-d Slater integrals. This can be seen in the picture 3. There are

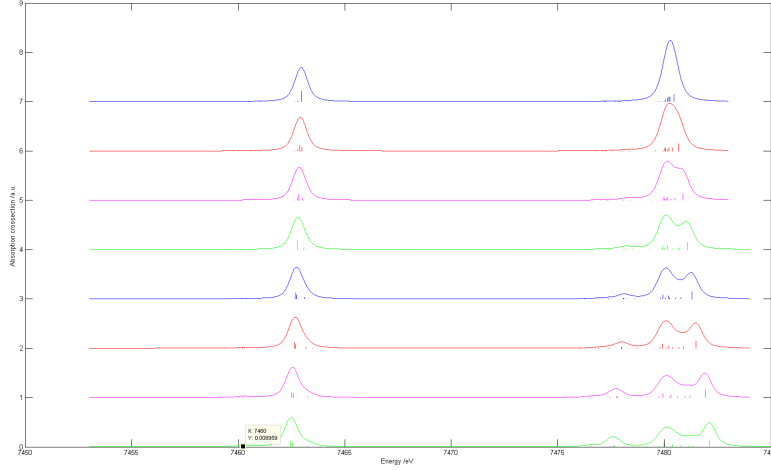


Figure 2: Energy level increasing from 0.1 (top) to 0.8 (bottom) the value of p-d interactions

as expected 4 peaks (because of the 4 possible couplings of  $^3F$  with  $p_{\frac{3}{2}}$ ) with the correct ratios 6 : 8 : 10 : 12. The structure is quickly lost as the interaction between orbitals is increased and new peaks arise 2. The new peak

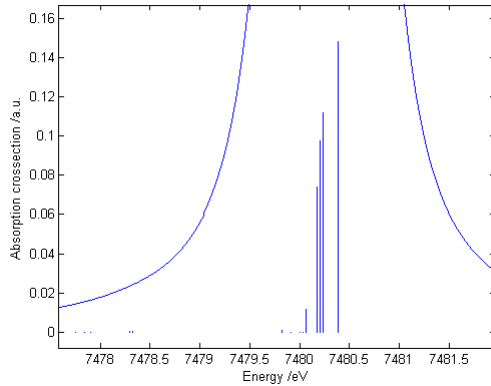


Figure 3: 4 levels for the  $K_{\alpha 2}$  part of the spectrum: the slater integrals reduction is set to 0.06, it can be seen that there's a new, still low level, coming up

arising is probably still the  $^3P$  which couples with the core hole  $^2P_{\frac{3}{2}}$ . In the end, with the p-d interaction set to 1, we get 6 main peaks in the central zone which are 4 from the original 4-plet of  $^3F_4$  and two are the allowed peaks with final valence orbital  $^3P_2$ , because it can have as final total angular momentum  $J = 2 + \frac{3}{2}, 2 + \frac{1}{2}, 2 - \frac{1}{2}, 2 - \frac{3}{2}$ . Since the possible initial ang momenta are  $J = \frac{9}{2}, \frac{7}{2}$  (that have the same energy, since they only differ for the S-shell spin), only the first 2 final states are possible. Because of L-S coupling there are, in the end, a lot of smaller peaks 4.

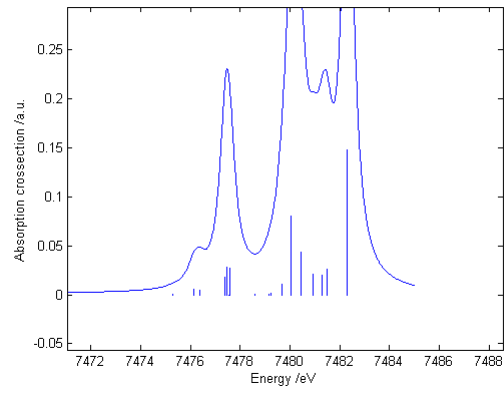


Figure 4:  $K_{\alpha 2}$  peaks with slater integral reduction set to 1 (80% of normal value)

## 6.2 Crystal field

### 6.2.1 $K_\alpha$

I now introduce the crystal field parameters in the simulations. Looking at the single electron levels, with any of the 3 sets of parameters found on internet, the LUMO is always the  $b_{1g}$  level, which correspond to the  $d_{x^2-y^2}$  orbital. This is considering the case of strong ligand field, thus using the base of the  $D_{4h}$  repr.

In the very strong crystal field case, which is not this case, the  $p_{\frac{1}{2}}$  is not split, since the  $d_{x^2-y^2}$  orbital interacts differently only with the  $m = \pm 1$  or  $m = 0$  p levels and  $p_{\frac{1}{2}}$  only contains  $m = \pm 1$  levels.  $p_{\frac{3}{2}}$  instead is split in 2 levels, with a separation of  $\approx 1\text{eV}$  and a branching ratio which is theoretically 1:1. This can be seen in the following picture 5, where the parameters are set

$$D_q = 0.93 \quad D_s = 0.93 \quad D_t = 0.75$$

which is 3 times their actual value. If the cristal field is decreased to his normal value the number of peaks greatly

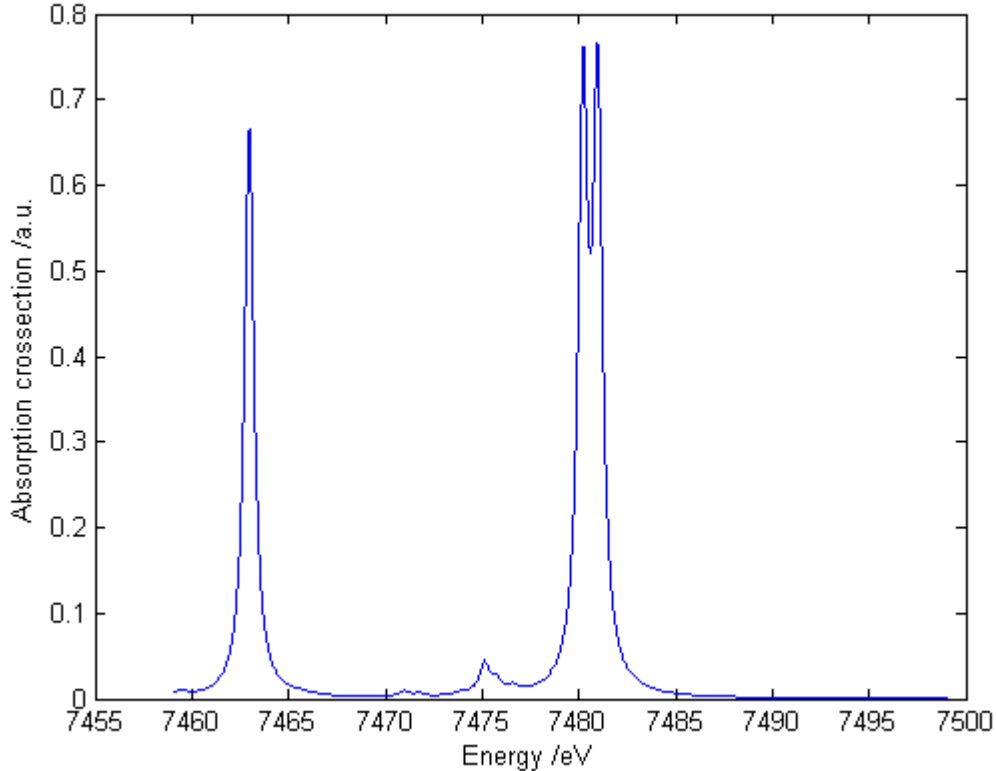


Figure 5: Spectrum in presence of very strong cristal field

increases.

### 6.2.2 $K_\beta$

In presence of pure Octahedral field, one can observe 3 main peaks (ignoring all the LS coupling)6.

The smaller peaks observed are mostly due to transitions in the  $-4D_q$  levels. The high peak with the lowest energy is due to both holes being on the  $a_{1g}$  level. This because if we introduce a small  $D_s$  parameter, it can be seen that this level increases its energy.

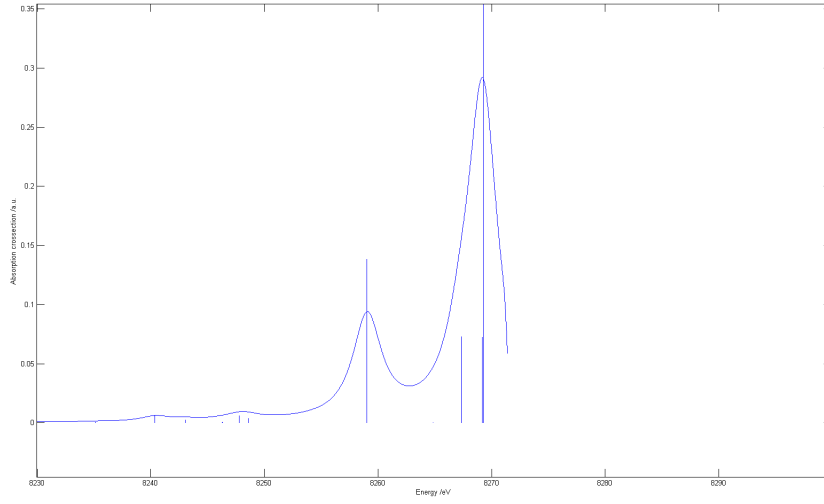


Figure 6: Spectrum of  $K_{\beta}$  in presence of a pure octahedral field with LS coupling turned off

### 6.3 Crystal field parameters for high-low spin state

The ground state is high spin if the crystal field splitting is not too high, which typically happens when the coupling energy is higher than the separation due to the crystal field of the  $E_g$  levels, that are split because of  $D_s$  and  $D_t$  into  $a_{1g}$  and  $b_{1g}$ . Doing test with CTM, this happens when the separation of between the LUMO and the HOMO is about of  $\Delta E \approx 3\text{eV}$  (it varies beacause of the different couplings with the  $p$  orbital and the  $d$  modified orbitals).

Now I test trying to increase the parameters to force the system in the low spin state (the high spin is achieved with low parameters).

For  $D_q = 0.3\text{eV}$ ,  $D_t = 0\text{eV}$  the transition occurs at  $D_s = 0.77\text{eV} \rightarrow 0.78\text{eV}$  Which means, considering the single energy levels, that the gap has to be around  $2.7\text{eV}$ .

The simulations are shown below If instead we higher the parameter from 0 to  $D_t = 0.22$ , we observe a transition

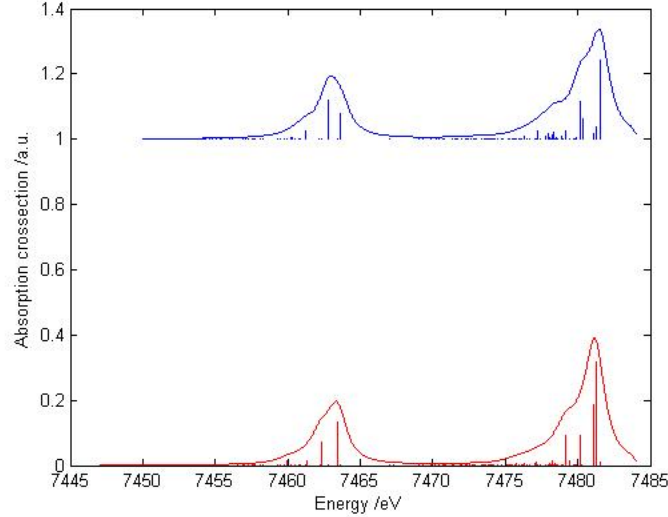


Figure 7:  $D_s$  parameter set to 0.77 (above) and 0.78(below)

sooner, for  $D_s = 0.38\text{eV} \rightarrow D_s = 0.39\text{eV}$

This is shown in the following picture:

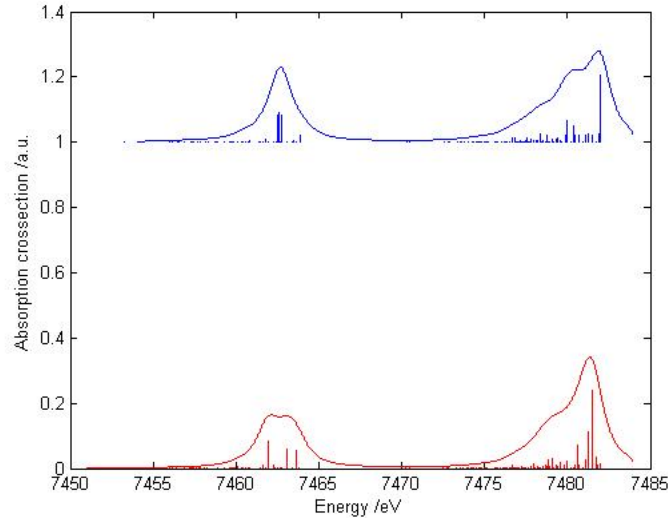


Figure 8:  $D_s$  parameter set to 0.48 (above) and 0.49(below)

For a pure octaedral complex, it's interesting to see how much the crystal field affects the spectrum; for a very slight field (around  $D_q = 0.05\text{eV}$ ) the free atom levels are basically split in a lot of new levels and the field is not strong enough to select only certain levels, so they are all mixed together and the spectrum is very wide.

With the increase of the field, one can see that the molecule starts doing transition only with certain levels selected by

the field (on the  $K_{\alpha 1}$  one can see, for example, 2 main levels) and which basically consist of the different arrangement of the outer orbital with respect to the  $p$  orbital.

After a certain value, in which we force the valence orbitals to remain in the HOMO, increasing the field doesn't affect the figure anymore. This can be seen in the following figure 9.

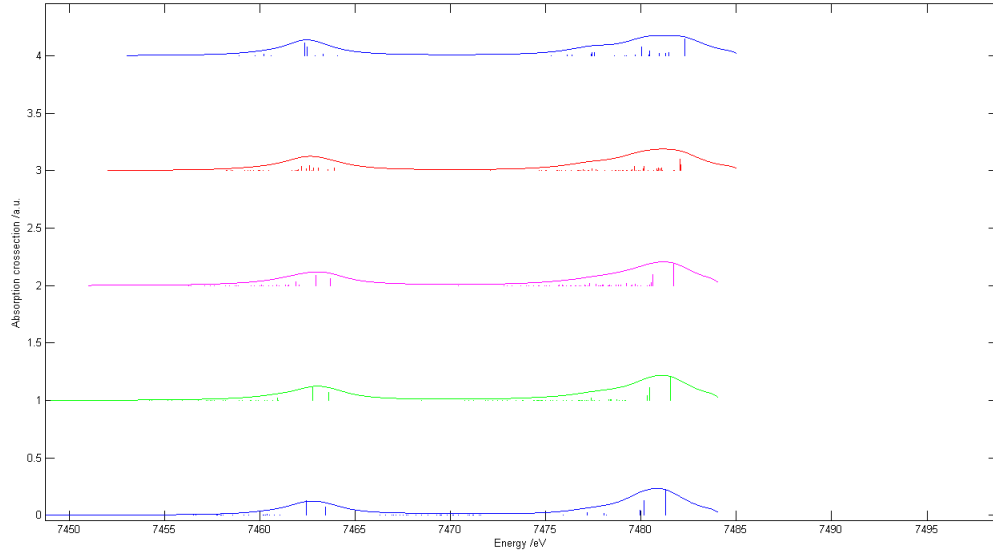


Figure 9: the crystal splitting parameter  $10D_q$  is set, from up to down, to 0-0.5-1.6-2.7-10 eV; apart from an energy shift, there's not much difference between the 2.7 and the 10 spectrum

Let's focus now on the  $K_\beta$  edge for Nickel. As noticed the high spin-low spin transition occurs more or less for the same crystal field parameters. In the high spin case, a pre-edge structure can be seen, this is because, when the atom has all of the orbitals available, it can move electron in a more favorable distribution according to the attraction with the core hole.

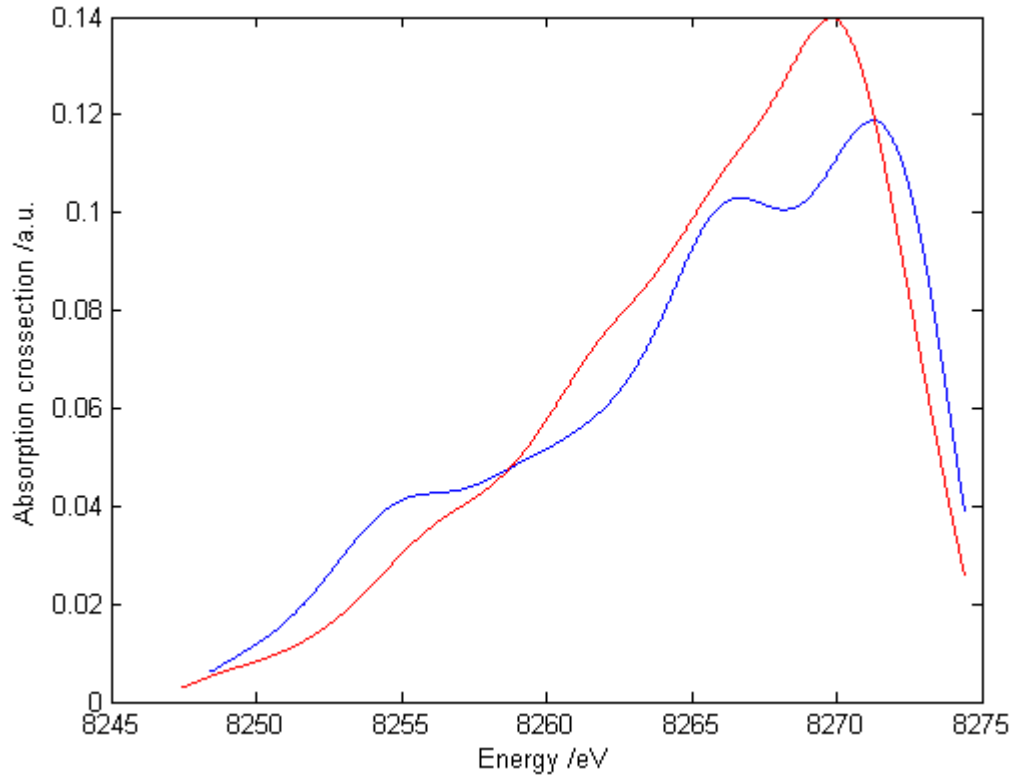


Figure 10: In red there is the low spin state, with field parameters (in eV)  $D_q = 0.27$   $D_t = 0.22$   $D_s = 0.49$ , in blue there is the high spin state with the pre-edge structure, with field parameters:  $D_q = 0.27$   $D_t = 0.22$   $D_s = 0.48$  both figure have Lorentian broadening of 2eV and Gaussian broadening of 1 eV



Also it's convenient to reproduce the same graph as 9 but with  $K_\beta$  emission lines and see if more or less all the high spin states have the same shape. The results are plot in fig 11

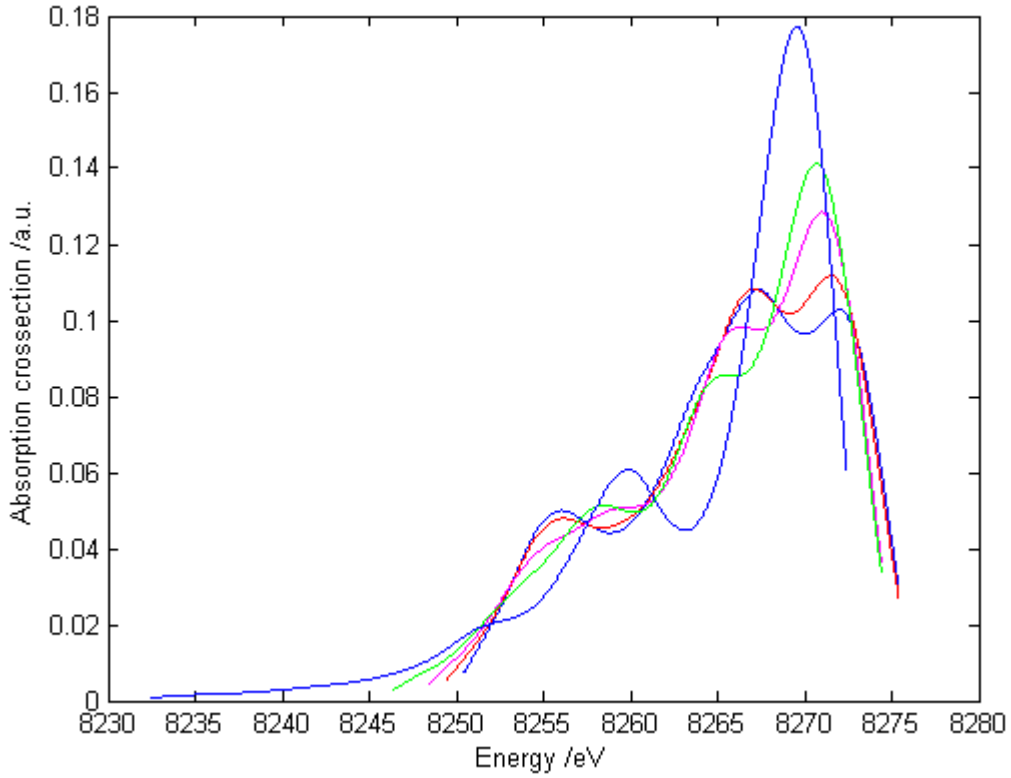


Figure 11: The Lorentian and Gaussian broadening are set on 2 and 1 eV respectively, the  $10D_q$  gap is increased from  $0\text{eV} \rightarrow 0.5\text{eV} \rightarrow 1.6\text{eV} \rightarrow 2.7\text{eV} \rightarrow 10\text{eV}$  one can see there is always the smaller peak before the big one

The pre peak in the high spin state can be explained as follow; first of all we note that a pre peak means an initial state with higher energy, since it is the initial state that changes with the transition. The other thing to note is that when we have 2 electrons, they repel more each other if they have opposite spin, since there is no contribution from the negative exchange integral. If we have an electron and a hole, the situation is the opposite, so when we have a high spin state, the  $s$  hole spin can be aligned with the spin of the molecule or opposite, which can make it feel more or less the attraction of the valence electrons.

## 7 fit results

### 7.1 Ni(Pc)

Ni(Pc) (Nickel Phtalocyanine) is a metal complex where the nickel central atom has oxidation number 2+ and has bound with four Nitrogen atoms.

This is the typical shape with  $D_{4h}$  exact symmetry, at least as long as we only consider one molecule at the time.

#### 7.1.1 $K_\beta$ emission lines

Now I try to compare the results of the fit with the data of NickelPhtalocyanine. The data I got were obtained at XFEL, and are plotted in the figure 14

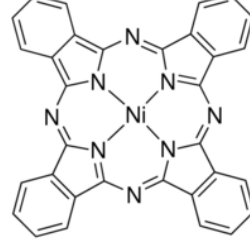


Figure 12: Shape of NiPc molecule

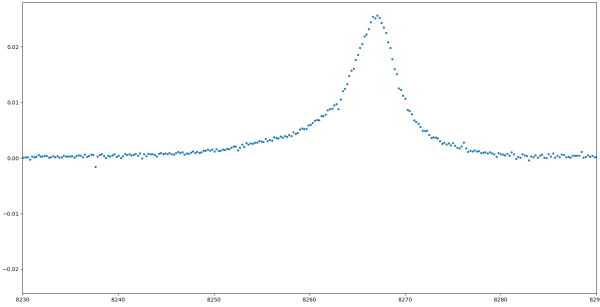


Figure 14: XFEL data of the NiPc compound

It's already clear that the parameter found on [4] won't fit, for the Kbeta emission lines, since they present a two very high peaks structure that are not present in the experimental data, as reported in figure 15.

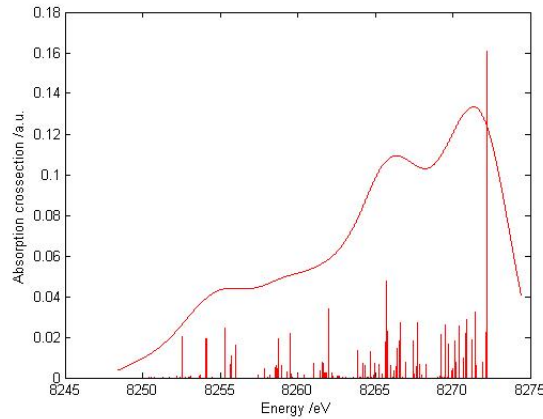


Figure 15: Obtained simulated Xes with the crystal field in [4], that is  $D_q = 0.27$ ,  $D_s = 0.37$ ,  $D_t = 0.22$ , Just as seen in section, this kind of field produces two high peaks in the Xes Kbeta lines, and the height of the second peak on the left is decreased as  $D_q$  is increased (as shown also in fig11)

As sad in \*the caption of figure 15, one has to increase the  $D_q$  field to make the main peak higher. For a very strong ligand field (I am using  $10D_q = 9\text{eV}$ , which is 3 times more of the typical electron coupling energy as seen in the following lines), the second peak more or less becomes  $\frac{1}{3}$  of the main one, which can also be seen in Figure 11. The only way to make the second peak much smaller than the

first one is to go from a high spin configuration. To achieve this, I notice that the gap between the first two highest energy levels (which are the lowest energy levels if we switch from the electron picture to the hole picture) is , in the case of strong  $D_q$ ,  $4D_s + 5D_t$ .

As long as this gap is more that  $\approx 3.1\text{eV}$ , the spectrum changes abruptly, which means there is a transition, and this can only mean that the 2 valence holes, from being in the  $b_{1g}$  and  $a_{1g}$  levels, are then only in the  $b_{1g}$  level, which results in a low spin state.

An example of such transition is reported in the following picture 16.

Here, I actually try to fit it, obtaining decent results 17.

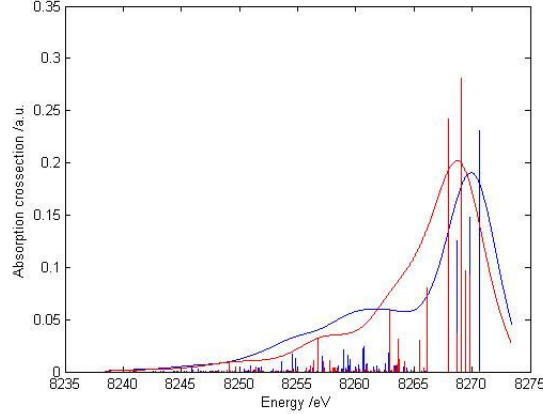


Figure 16: This is the transition , that occurs with very strong  $D_q = 0.9\text{eV}$  and  $D_s = 0.4\text{eV}$  and  $D_t = 0.3\text{eV}$  (blue)  $\longrightarrow$   $0.32\text{eV}$  (red) It's clear that the red figure is much closer to the data, also it has all the strong transitions much closer to the main transition, which results in a broader and higher main peak.

The fit has been carried out using the *scipy.optimize* function from the scipy package. The transition lines have been obtained using the output *\_sticks.xy* from the CTM4XAS program. This output file is only present with the option suppressed stick unticked, because it's only used by the matlab program to plot the sticks. Must be said that for some reason the energy transition are different in this output file from what the CTM program actually plots, with the following relation

$$E_{\text{outputfile}} = \text{constant} - E_{\text{plotted}}$$

This thing can be easily handled with the fit, adding a parameter for the shift in energy of the whole spectrum to get the constant. The most relevant parameters for both fit are just the lorential (HWHM) and gaussian broadening.

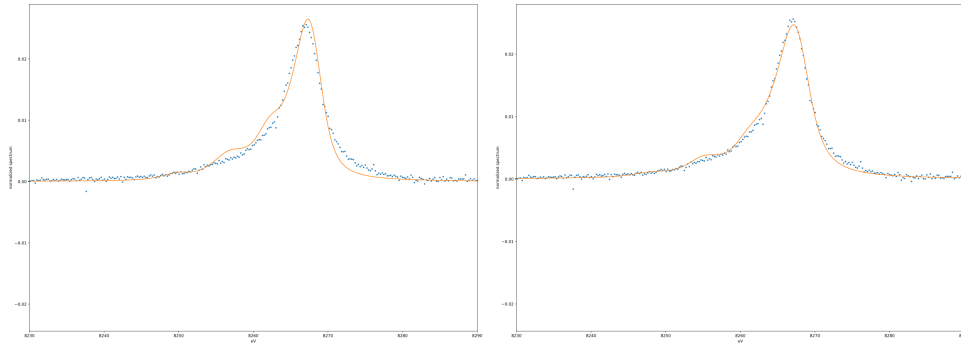


Figure 17: Two attempts of fitting the data, with plot obtained with crystal field parameters  $D_q = 0.7\text{eV}$ ,  $D_s = 0.41\text{eV}$  and  $D_t = 0.3\text{eV}$  on the left and  $D_q = 0.9\text{eV}$ ,  $D_s = 0.42\text{eV}$  and  $D_t = 0.3\text{eV}$ , one can see very clearly how increasing the  $D_q$  field reduces the height of the second peak. Also, this spin configuration is the right one for the program, since the structure of the spectrum is the same of the data. The main difference are the fact that the two smaller peaks on the left are lower in the data, but present nevertheless.

They are:

$$\sigma = 1.49\text{eV} \quad \Gamma = 1.10\text{eV}$$

for the fit 17 on the left and:

$$\sigma = 1.06\text{eV} \quad \Gamma = 1.61\text{eV}$$

for the one on the right.

### 7.1.2 $K_\alpha$ emission lines

After fitting the  $K_\beta$  spectrum, that has a much richer structure, which allows us to find the optimal field parameters, it's turn for the  $K_{\alpha 1}$  and  $K_{\alpha 2}$  lines. The wider fine structure separation allows us to distinguish them and this is because the  $2p$  orbital is much closer to the center than the  $3p$  one, and hence has a stronger L-S coupling. For coherence, I must try to fit the data with the parameters I used in the previous section:

$$D_q = 0.7\text{eV} \quad D_s = 0.41\text{eV} \quad D_t = 0.3\text{eV}$$

$$D_q = 0.9\text{eV} \quad D_s = 0.42\text{eV} \quad D_t = 0.3\text{eV}$$

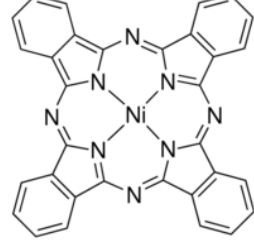


Figure 13: Shape of NiPc molecule

From theory we know that the lorentian broadening has to be the same as in the  $K_\beta$  emission lines, since they are both produced by the decay of the same  $1s$  core hole state, so it won't be a fit parameter. The result can be seen in the following picture:

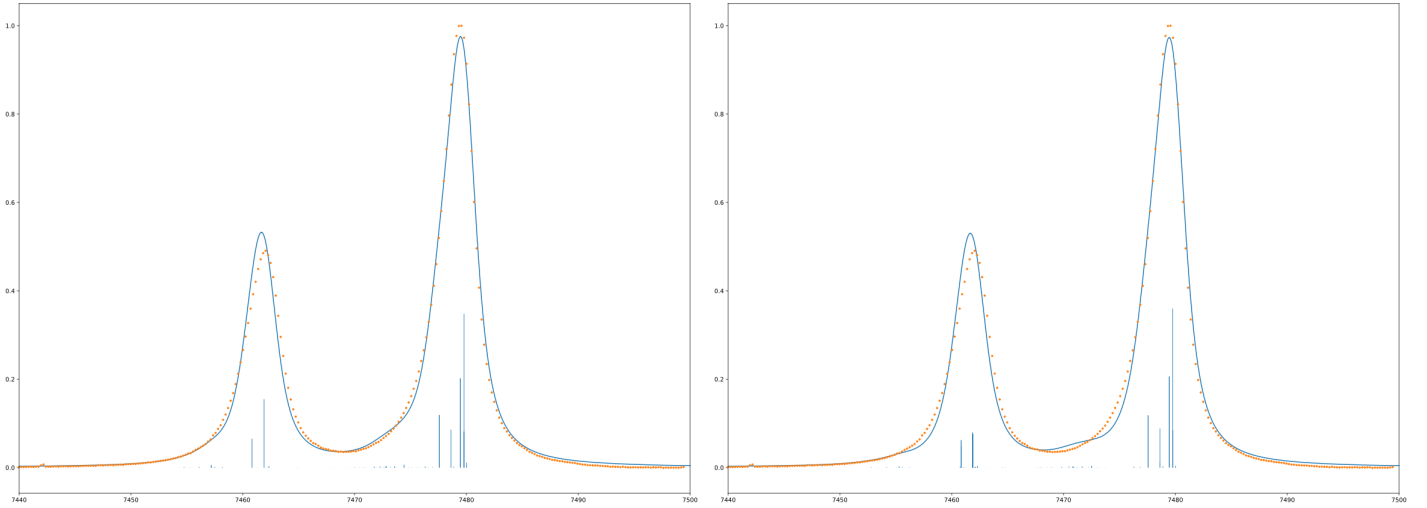


Figure 18: on the left the fit with  $D_q = 0.7\text{eV}$ , on the right the one with  $0.9\text{eV}$ . This time, the agreement is better for the graph on the left, because the other one substantially fails to get the right  $K_{\alpha 1}$  and  $K_{\alpha 2}$  separation, but more or less all the transitions are of the same intensity.

If we try to lower the crystal field to fall again in the case of low spin, we find that there is not a big difference in the spectrum, since in the  $K_\alpha$  emission lines, all the lines are very close together (except for the fine structure separation).

This is due to the fact that the influence of the valence shell, is much weaker in this case.

The spectrum without crystal field is more or less the same, it mostly changes only the relative heights of the peaks.

## 7.2 Ni(Terpy)<sub>2</sub>

The Ni(Terpy)<sub>2</sub> molecule has not a perfect  $O_h$  symmetry, nor a  $D_{4h}$  symmetry, because it is made of these two ligand that arrange around the Ni atom in an Octahedral way, since there are 6 N atoms, but not exactly Octahedral. Nevertheless, we expect the compound to be in a high spin configuration, since its departure from  $O_h$  symmetry should be low. In fact, any Ni<sup>2+</sup> complex with Octahedral field is supposed to be in a high spin configuration, since all the energy levels are degenerate with this symmetry and so one can't find the two holes in same orbitals, since there's no energy gap to compensate the pairing energy.

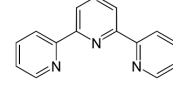


Figure 19: Shape of Terpy Ligand

### 7.2.1 $K_\beta$ emission lines

As before I start with the  $\beta$  emission lines since it has more information contained. The data for this complex has been obtained both at XFEL and P64 and the acquisitions look very similar. If I try to fit with a high spin state, though, the agreement is very poor, as can be seen in the following picture 20. Instead it is clear that the low spin fit

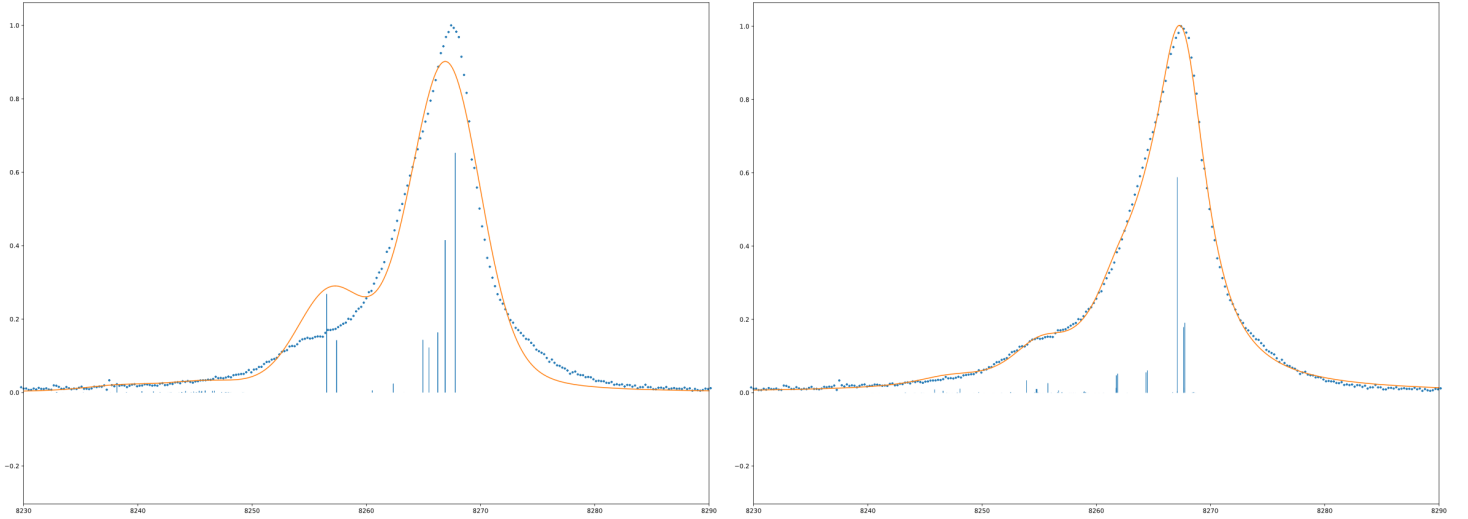


Figure 20: These are the plots obtained with Xes in the case of high(left)/low(right) spin. The Crystal field parameters used are  $D_q = 1\text{eV}$ ,  $D_s = 0.5\text{eV} \rightarrow 0.53\text{eV}$  and  $D_t = 0.22\text{eV}$

is in very high agreement with the data.

The fit parameter are (for the fit on the right)

$$\sigma = 0.65\text{eV} \quad \Gamma = 2.38\text{eV}$$

This is very weird because to achieve such a state, there should be a strong departure from the  $O_h$  symmetric field, which is not the case of a Terpyridine.

It may be possible that the ligand field also interferes with the  $3p$  orbital, which is very close to the outer shell, thus distorting the normal high spin spectrum. In fact, changing (a lot) the Slater reduction parameters, it is possible to reduce the height of the peak on the left that can be seen in the high spin plot, which physically can be a consequence of the distortion of the orbital due to both the crystal field and the presence of the core-hole (in fact, the reason for the Slater integrals in Xas are usually rescaled to 80% of their normal value is to account for the hole in the p-shell).

### 7.2.2 $K_\alpha$ emission lines

In this case, instead, the emission lines is fit well in the presence of a pure octahedral field, but this might just be due to the very simple structure of the  $K_\alpha$  emission lines.

The fit parameters obtained are, in the end:

$$\sigma = 0.9\text{eV} \quad \gamma = 0.89\text{eV}$$

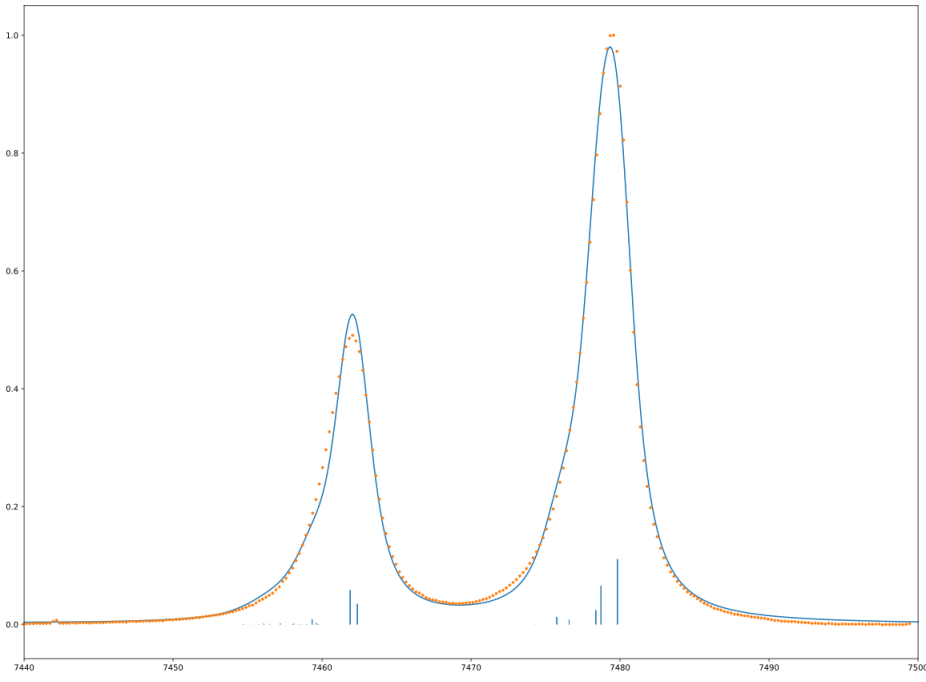


Figure 21: Fit obtained with the field parameter  $D_q = 3\text{eV}$

Must be noticed that there's very poor agreement between the  $\Gamma$  value calculated with the  $K_\beta$  emission lines.

## 8 ORCA programm

I also used an ab-initio program, called Orca, to estimate the  $K$  emission lines but the result weren't satisfying. This because the program uses the TDDFT (time dependent density functional theory) method to proceed with the calculation, which cannot account for the rich multiplet structure of the transition. For completeness, here there are the plots obtained:

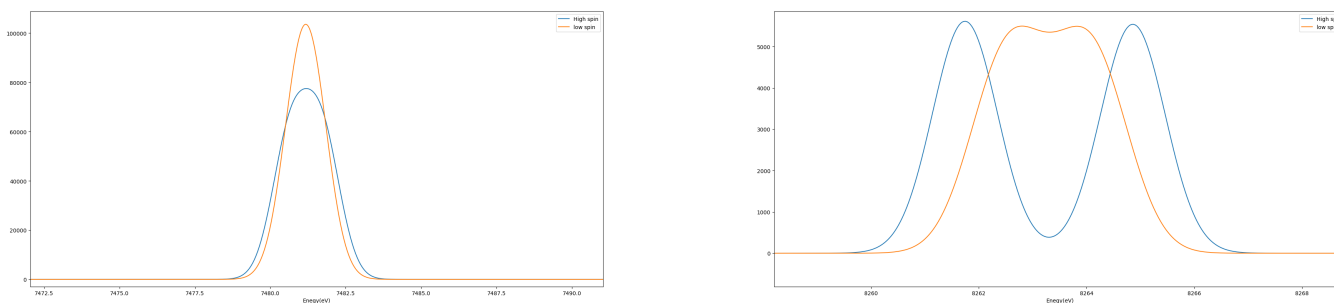


Figure 22: Orca simulated spectra of  $\alpha$  (left) and  $\beta$  (right) emission lines. As can be seen, there's very little agreement with the data because the multiplet structure is missing, but the energies of the transitions are the right ones.

## References

- [1] C. J. BALLHAUSEN, *Introduction to LIGAND FIELD THEORY*. MCGRAW-HILL BOOK COMPANY, INC., 1962.
- [2] M. W. H. Patric Zimmermann, Robert J. Green and F. M. F. de Groot, "Quanty4rixs: a program for crystal field multiplet calculations of rixs and rixs-mcd spectra using quanty," *Journal of Synchrotron Radiation*, 2018.
- [3] J. Telser, "A perspective on applications of ligand-field analysis: inspiration from electron paramagnetic resonance spectroscopy of coordination complexes of transition metal ions," *Journal of the Brazilian Chemical Society*.
- [4] C. K. K. N. J. J. I. B. F. J. H. Phillip S. Johnson, J. M. García-Lastra and P. L. Cook, "Crystal fields of porphyrins and phthalocyanines from polarization-dependent 2p-to-3d multiplets," *The Journal of Chemical Physics*.